Since January 2020 Elsevier has created a COVID-19 resource centre with free information in English and Mandarin on the novel coronavirus COVID-19. The COVID-19 resource centre is hosted on Elsevier Connect, the company's public news and information website.

International Immunopharmacology 13 (2012) 331–340

Contents lists available at SciVerse ScienceDirect

International Immunopharmacology

journal homepage: www.elsevier.com/locate/intimp

Houttuynia cordata inhibits lipopolysaccharide-induced rapid pulmonary fibrosis by up-regulating IFN-γ and inhibiting the TGF-β1/Smad pathway

Shaohui Du [a,1,*], Hui Li [b,1], Yinghai Cui [c], Lina Yang [a], Jingjing Wu [b], Haiyuan Huang [b], Yangyan Chen [a], Wei Huang [a], Rong Zhang [a], Jun Yang [a], Dongfeng Chen [b], Yiwei Li [b], Saixia Zhang [b], Jianhong Zhou [b], Zhijun Wei [b], Ngai Tan Chow [d]

[a] *Department of Internal Medicine, Affiliated Shenzhen Hospital, Guangzhou University of Chinese Medicine, Shenzhen 518033, China*
[b] *Department of Anatomy, Guangzhou University of Chinese Medicine, Guangzhou 510006, China*
[c] *Department of Respiratory Medicine, The Second Affiliated Hospital, Liaoning University of Traditional Chinese Medicine, Shenyang 110034, China*
[d] *The Chinese University of Hong Kong, Hong Kong, China*

ARTICLE INFO

Article history:
Received 4 December 2011
Received in revised form 6 March 2012
Accepted 15 March 2012
Available online 2 May 2012

Keywords:
Houttuynia cordata vapor extract
Lipopolysaccharide
Rapid pulmonary fibrosis
IFN-γ
TGF-β1

ABSTRACT

This study aimed to explore the effect and mechanism of *H. cordata* vapor extract on acute lung injury (ALI) and rapid pulmonary fibrosis (RPF).

We applied the volatile extract of HC to an RPF rat model and analyzed the effect on ALI and RPF using hematoxylin–eosin (H&E) staining, routine blood tests, a cell count of bronchoalveolar lavage fluid (BALF), lactate dehydrogenase (LDH) content, van Gieson (VG) staining, hydroxyproline (Hyp) content and the dry/wet weight ratio. The expression of IFN-γ/$STAT_1$, IL-4/$STAT_6$ and TGF-β_1/Smads was analyzed using ELISA, immunohistochemistry and western blotting methods. The active ingredients of the HC vapor extract were analyzed using a gas chromatograph–mass spectrometer (GC–MS), and the effects of the active ingredients of HC on the viability of NIH/3T3 and RAW264.7 cells were detected using an MTT assay.

The active ingredients of the HC vapor extract included 4-terpineol, α-terpineol, L-bornyl acetate and methyl-n-nonyl ketone. The results of the lung H&E staining, Hyp content, dry/wet weight ratio and VG staining suggested that the HC vapor extract repaired lung injury and reduced RPF in a dose-dependent manner and up-regulated IFN-γ and inhibited the TGF-β1/Smad pathway *in vivo*. *In vitro*, it could inhibit the viability of RAW264.7 and NIH/3T3 cells. It also dose-dependently inhibited the expression of TGF-β1 and enhanced the expression of IFN-γ in NIH/3T3.

The HC vapor extract inhibited LPS-induced RPF by up-regulating IFN-γ and inhibiting the TGF-β1/Smad pathway.

1. Introduction

Traditionally, acute lung injury (ALI) causes pneumonedema and matrix lesions, rather than pulmonary fibrosis [1,2]. However, the common characteristics of some new diseases, such as severe acute respiratory syndrome (SARS) first studied in 2003, avian influenza first studied in 2008, and the swine influenza pandemic first studied in 2009, suggest that ALI may initiate these pathologies, and in acute respiratory distress syndrome (ARDS) with rapid pulmonary fibrosis (RPF), ALI can be the most important lethal factor in the short-term [3]. Acute exacerbations of idiopathic pulmonary fibrosis and the mechanisms of repair and remodeling in acute lung injury have recently gained much attention [1,4–6]. Based on the common characteristics and mechanisms of these diseases, we established a new RPF model that could be induced by ALI *via* a lipopolysaccharide (LPS) three-hit regimen and found that days 3–7 and 14–21 were two important time windows for RPF.

Houttuynia cordata (HC), a grass of the Saururaceae *H. cordata* thumb, is a promising drug for treating RPF. The Chinese Health Department and a clinical report claimed that HC could prevent and treat SARS [7] and avian influenza [8,9]. HC water extracts had immunomodulatory and anti-SARS activities, as evidenced by the ability to significantly inhibit SARS-CoV 3C-like protease and RNA-dependent RNA polymerase [10], which significantly and dose-dependently stimulated the proliferation of mouse splenic lymphocytes and increased the proportion of $CD4^{(+)}$ and $CD8^{(+)}$ T cells and the secretion of IL-2 and IL-10. The HC ethanol extract inhibited the expression of

* Corresponding author at: Department of Internal Medicine, Affiliated Shenzhen Hospital, Guangzhou University of Chinese Medicine, No. 2 FuhuaRoad, Shenzhen518033, China. Tel.: +86 013312991354; fax: +86 755 88359333.
E-mail address: dushaohui@tom.com (S. Du).
[1] Shaohui Du and Hui Li are the first authors because they contributed equally to this study.

1567-5769/$ – see front matter © 2012 Elsevier B.V. All rights reserved.
doi:10.1016/j.intimp.2012.03.011

IL-4 and IL-5 and the migration of TARC-induced Jurkat T cells. The injection of HC had a direct inhibitory effect on Pseudorabies herpesvirus (PrV) *in vitro* [11], and HC was shown to be a selective COX-2 inhibitor [12]. The volatile chemical components of HC are its main pharmacologically active components [13,14]. Therefore, the volatile extract of HC might be an alternative drug for treating RPF.

The injection of HC produced from the volatile extract was suspended by the State Food and Drug Administration of China (SFDA) due to reports of allergic shock between 2006 and 2008; however, the use of Tween 80 as an adjuvant solution for the HC extract might be the primary cause of the reported allergic shock [15]. Afterwards, the SFDA re-approved the use of HC intramuscular injections and strengthened the standardization of its production and quality management to improve security. The research into HC active ingredients and their pharmacological mechanisms is indispensable.

2 . Materials and methods

2.1. Materials

LPS (O555:B5) and dexamethasone (Dex) were purchased from Sigma (St. Louis, United States). HC vapor extract (999 Enterprise Group, China) was prepared as follows: fresh HC (2000 g) was exposed to steam distillation. The forerunning liquid (200 ml) was collected for redistillation. Then, 7 g of sodium chloride was added to the redistilled liquid (1000 ml).

2.2 . Animals and treatment

A total of 315 healthy Wistar rats (200 to 220 g, half male and half female) supplied by the Experimental Animals Center of Guangzhou University of Chinese Medicine were randomly allocated into 6 groups: 1) control group (n = 35); 2) LPS group (n = 56); 3) Dex group (n = 56); 4) group that received a high dose of HC (H-HC group, 16.5 mg/kg) (n = 56); 5) group that received a medium dose of HC (M-HC group, 10 mg/kg) (n = 56); and 6) group that received a low dose of HC (L-HC group, 3.5 mg/kg) (n = 56).

2.3 . Ethical handling of animals

All experiments were conducted in strict accordance with the recommendations in the Guide for the Care and Use of Laboratory Animals of the National Institutes of Health. The protocol was approved by the Committee on the Ethics of Animal Experiments of Guangzhou University of Chinese Medicine. All surgery was performed under sodium pentobarbital anesthesia, and efforts were made to minimize suffering.

A detailed description of the model was published previously [16]. First, the rats were given LPS (1.5 mg/kg) intratracheally. After 24 h, LPS (3 mg/kg) was given intraperitoneally, and 48 h later, LPS (3 mg/kg) was given intratracheally. Two acute stages of development of pulmonary fibrosis were observed on days 7 to 9 and on days 14 to 21. After the rats received the third LPS administration, Dex (3 mg/kg) and HC were administered intraperitoneally once a day for 7 days. High, medium and low dosages of HC were determined on the basis of the clinical application in adults according to the FDA guidelines for industry and reviewers for estimating the safe starting dose in clinical trials for therapeutics in adult healthy volunteers. The collection of samples for testing began on day 1 (24 h after completing the third LPS administration). Blood and lung tissue samples were taken on days 1, 3, 7, 14, 21, and 28.

2.4 . Testing lung tissue samples for hematoxylin–eosin (H&E) staining and van Gieson (VG) staining

The rats were infused with 4% paraformaldehyde to fix the tissue. The middle lobes of the right lung were embedded in paraffin and sliced into 5 μm sections for H&E and VG staining.

2.5 . Testing blood samples, bronchoalveolar lavage fluid (BALF) cell counting, and determining lung dry/wet weight

Blood and BALF samples from the right basement trunk were used for cell counting and lactate dehydrogenase (LDH) testing. The samples were analyzed by the laboratory of the First Affiliated Hospital of Guangzhou University of Traditional Chinese Medicine. Serum cytokines were analyzed using an enzyme-linked immune-absorbent assay (ELISA). Tissue (100 mg, wet weight) from the same location was dried until a constant weight (dry weight) was obtained. The dry weight subtracted from the wet weight indicates the water content, representing the level of inflammation, and the dry/wet weight ratio is the lung parenchyma weight ratio, representing the level of fibrosis. The extracted total protein of the lung was preserved with protease inhibitors (Calbiochem) for the western blotting assay.

2.6 . Pulmonary hydroxyproline (Hyp) content

Wet tissue (100 mg) from the middle lobe of the right lung was used to determine hydroxyprolone (Hyp) content using the alkaline hydrolysis kit (Jiancheng Bioengin., Nanjing, China).

2.7 . ELISA

The expressions of IFN-γ, IL-4, and TGF-β1 in the plasma from rats and the supernatant from cell lines were investigated using an ELISA kit (Zymed, Invitrogen, USA). The absorbance at 450 nm was analyzed using an Elx 808^{TM} absorbance microplate reader (Bio Tek, USA).

2.8 . Immunohistochemistry

Endogenous peroxidase was extracted with 3% hydrogen peroxide (H_2O_2, 30 min), and the sections were blocked with blocking buffer (5% BSA and 0.03% Triton X-100 in phosphate-buffered saline) at 37 °C for 30 min. The samples were then incubated with monoclonal anti-IFN-γ, anti-IL-4, anti-TGF-β1/TGF-β receptor I, Smad2/3, Smad4, and Smad7 antibodies (all from Santa Cruz, USA) or an anti-α-SMA antibody (Abcam, Cambridge) at 37 °C for 2 h or at 4 °C for 18 h. Then, the sections were incubated with a secondary antibody at 37 °C for 1 h, followed by incubation with horseradish peroxidase (HRP)-labeled Vectastain Elite ABC reagent (Vector Laboratories) at 37 °C for 1 h. Horseradish peroxidase binding was detected in 0.005% diaminobenzidine (DAB) and 0.01% H_2O_2.

2.9 . Western blotting

The extracted protein samples from the lungs and cell lines were separated by SDS-PAGE (12% acrylamide) and transferred onto a PVDF membrane at 0.8 mA/cm^2 for 2 h. The membrane was blocked with 5% nonfat milk dissolved in 20 mM Tris–HCl (pH 7.4) containing 150 mM NaCl and 0.05% Tween 20 (TBS-T). The membranes were washed with TBS-T and incubated with monoclonal anti-IFN-γ, anti-IL-4, anti-TGF-β1/TGF-β receptor I, anti-Smad2/3, anti-Smad4, anti-Smad7 (all from Santa Cruz, USA), anti-STAT1 (Abcam, Cambridge), anti-STAT6 (Cell Signaling Technology, USA) and anti-β-actin (Sigma, USA) antibodies at 37 °C for 2 h. Finally, the membranes were treated with HRP-conjugated IgG (Sigma, USA) and detected by enhanced chemiluminescence (ECL western blotting substrate, Pierce Biotechnology, USA).

2.10 . GC–MS

The supernatant from the HC vapor extract was analyzed using an Agilent 6890 N + 5973 N GC–MS (USA) equipped with a 30 m × 0.25 mm × 0.25 μm DB-1MS quartz microcapillary chromatographic column (Agilent J&W Scientific) after extraction with 2 ml of cyclohexane and dehydrated alcohol demulsification. The GC oven temperature was held at 60 °C for 1 min, raised to 220 °C at 6 °C/min, and held for 3 min. The injector temperature was 250 °C, and the flow rate of the carrier gas, helium, was 1.3 ml/min at a 60:1 split ratio. The diluted samples (1.0 μl, 1/100 v/v, in ethyl acetate) were injected manually in the split mode. The major components of the HC vapor extract were identified by co-injection with standards wherever possible and confirmed with Kovats indices using the Wiley (V. 7.0) and National Institute of Standards and Technology (NIST) V2.0 GC–MS library. The relative concentration of each compound in essential oil was quantified based on the peak area integrated by the analysis program.

2.11 . Cell culture

Murine macrophage-like RAW 264.7 and embryonic fibroblast NIH/3T3 cells (Shanghai Institute of Cell Biology, The Chinese Academy of Sciences, Shanghai, China) were cultured in RPMI 1640 medium supplemented with 10% fetal bovine serum (FBS, Hyclone, Logan, UT), 100 U/ml penicillin and 100 mg/ml streptomycin in an atmosphere of humidified 5% CO_2 at 37 °C. At 80%–90% confluence, the RAW264.7 and NIH/3T3 cells were washed twice with, and subsequently cultured in, serum-free OPTI-MEMI medium (Invitrogen, Carlsbad, CA). After pre-incubation for 12 h, cell cultures were stimulated with LPS (100 ng/ml) and co-treated with the HC vapor extract and the active ingredients detected by GC–MS. Cell viability was determined with an MTT assay, and the levels of inflammatory cytokines, including IFN-γ, TGF-β1 and TNF-α, were determined using an ELISA assay.

2.12. Statistical analysis

Data were analyzed as the mean ± SD for each group. The difference between groups was analyzed with a factorial model ANOVA followed by Student's *t*-test. SPSS 11.5 (the software for statistical analysis) was used to perform all analyses, and $P<0.05$ was considered to be statistically significant.

3 . Results

3.1 . HC reduced ALI and RPF

3.1.1 . H&E staining

All H&E stained slides were examined by 3 investigators who were experienced in pneumonia pathology, and the majority decision was considered final (Supplement Table 1, Supplement Fig. 1A–T). The result showed that in the LPS group, there were a large number of monocytes and neutrophils in the alveolar spaces, and the alveolar inflammatory exudation was reduced in a dose- and time-dependent manner in the HC groups. The results suggest that HC vapor extract can reduce ALI.

3.1.2 . Cell counting analysis

Fig. 1A, Supplement Table 2: The lymphocyte ratio in the blood samples from the LPS group decreased from days 1 to 7 and returned to the same level as that of the control group on day 9. Compared with the LPS group, Dex reduced the lymphocyte ratio significantly ($P<0.01$); however, the levels in the three HC groups were significantly higher than those in the LPS and Dex groups on day 7 ($P<0.01$). The ratio of mononuclear phagocytes in BALF (Fig. 1B, Supplement Table 3) in the three HC groups on day 7 and day 14 was significantly higher than that in the LPS and Dex groups ($P<0.01$). The ratios changed in a dose-dependent manner. The results suggest that HC vapor extract can regulate the lymphocyte ratio.

3.1.3 . LDH in serum

Fig. 1 C, Supplement Table 4: LDH levels in all treatment groups were significantly lower than those in the LPS group ($P<0.01$). LDH levels in the HC groups were lower than those in the Dex group on day 14. The results suggest that HC can reduce ALI.

3.1.4 . Hyp content

Fig. 1D, Supplement Table 5: The Hyp content increased significantly in the LPS group ($P<0.01$) from day 3 to day 7 and from day 14 to day 21, representing two distinct RPF stages. The Hyp content in the H-HC group was significantly lower than that in the LPS and Dex groups on day 21 ($P<0.01$), indicating that the high-dose HC vapor extract had a better inhibitory effect on the later RPF stage.

3.1.5 . Lung dry/wet weight ratio

Fig. 1E, Supplement Table 6: Pulmonary fibrosis was inhibited on days 14–21 in a dose-dependent manner in the HC groups, and it was inhibited more significantly in the H-HC group. These results suggest that HC can reduce RPF.

3.1.6 . VG staining results

Fig. 2A–T: In the LPS group, collagen fibers were progressively deposited in the alveolar septum from days 1 to 28, and pulmonary consolidation was found on day 28 (Fig. 2A–D). Compared with the LPS group, fiber deposition was decreased in the Dex group (Fig. 2E–H). Compared with the Dex and LPS groups, fiber deposition was decreased significantly in the M-HC and H-HC groups on days 14 and 28 (Fig. 2, K > 2G > 2O > 2S and 2D > 2H > 2L > 2P > 2T). In addition, the decreasing of fiber deposistion in alveolar septum was consistent in the H-HC group was consistent with that in (Fig. 2T), suggesting that HC vapor extract might improve the alveolar framework and enhance alveolar ventilation. The results suggest that the HC vapor extract can reduce RPF in a dose-dependent manner.

3.2 . HC up-regulated IFN-γ expression on days 7–21

The serum ELISA results showed that IFN-γ expression decreased rapidly between days 1 and 7 and continued to decline gradually on day 14 in the LPS group (Fig. 3A, Supplement Table 7). IFN-γ expression decreased gradually from days 1 to 28 in the three HC groups, with the smallest decline observed in the H-HC group. The three HC groups showed high IFN-γ expression levels on days 7–21, suggesting that the HC vapor extract up-regulated IFN-γ secretion during days 7–21. This finding was consistent with the results of the western blotting (Fig. 4) and immunohistochemistry (Supplement Fig. 2) experiments and was further supported by the results from NIH/3T3 cells treated with HC. STAT1 is a downstream signaling molecule of IFN-γ. Western blotting results showed that STAT1 expression was synchronized with IFN-γ expression in all groups on day 1. However, the synchrony was disrupted on day 7. IFN-γ expression in the HC groups was higher than that in the LPS and Dex groups on day 7, and STAT1 expression in the HC groups was lower than that in the LPS and Dex groups on day 7 (Fig. 4), suggesting that HC might inhibit STAT1 expression through a non-IFN-γ pathway or that HC vapor extract might up-regulate IFN-γ expression through a non-STAT1 pathway.

3.3 . HC had the same effect as Dex on IL-4/STAT6 signaling

The serum ELISA results (Fig. 3B, Supplement Table 8) showed that IL-4 expression peaked on day 7 in all groups, which is consistent with the western blotting results. The western blotting results from the lung tissues (Fig. 4) showed that IL-4 expression was high

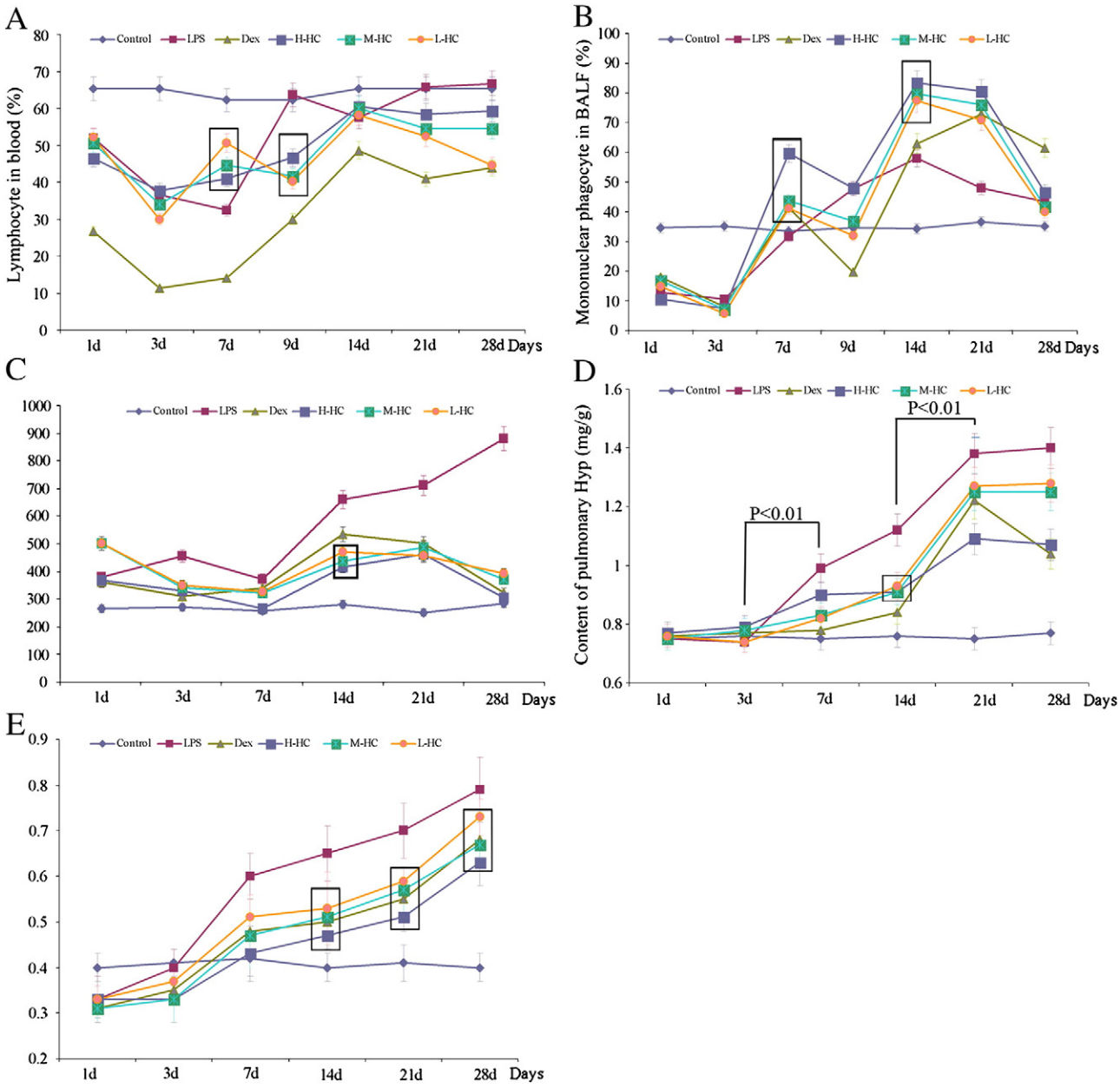

Fig. 1. Blood cell counts, LDH in serum, pulmonary Hyp content and lung dry/wet weight ratio. The statistical analysis is shown in supplementary Tables 2–6. The boxes in the figure highlight the dose-dependent trend of HC. There is a significant difference between the HC groups. (A) Lymphocytes in blood. (B) Monocyte count in BALF. (C) The content of LDH in the blood serum. (D) Content of pulmonary Hyp. (E) Lung dry/wet weight ratio.

in the LPS, Dex and L-HC groups but weak in the M- and H-HC groups on day 1. IL-4 expression increased on day 7 and decreased on day 28 in all groups. STAT6 expression (Fig. 4) changed along with IL-4 expression. There was no significant difference in IL-4 expression between the HC groups and the Dex group, suggesting that the HC vapor extract affected IL-4/STAT6 signaling in a similar manner as Dex.

3.4 . HC inhibited the TGF-β1/Smad pathway

The serum ELISA results showed that TGF-β1 expression increased from days 1 to 21 in the LPS group (Fig. 3C, Supplement Table 9). TGF-β1 expression in the Dex group was dramatically and persistently lower than that in the LPS group from days 1 to 28 ($P<0.01$). TGF-β1 expression in the HC groups increased from days 1 to 7 and decreased from days 7 to 28. The ELISA results showed that, compared with the LPS group, TGF-β1 expression in the HC groups decreased in a dose-dependent manner, which was consistent with the western blotting (Fig. 4) and immunohistochemistry (Supplement Fig. 2) results. Our results indicate that HC inhibited TGF-β1 expression. Smad2 and Smad3 (Smad2/3) are downstream signaling molecules of TGF-β1. The western blotting (Fig. 4) and immunohistochemical (Supplement Fig. 3) results showed that changes in Smad2/3 expression were consistent with the changes in TGF-β1 expression in all groups on days 1, 7 and 28.

Smad4 is the synergistic Smad of Smad2/3. The western blotting (Fig. 4) and immunohistochemical (Supplement Fig. 3) results showed that on day 1, Smad4 was expressed at high levels in all groups, with no significant differences among the groups. In the LPS and Dex groups, Smad4 expression was high on day 7, suggesting that Smad4 contributed

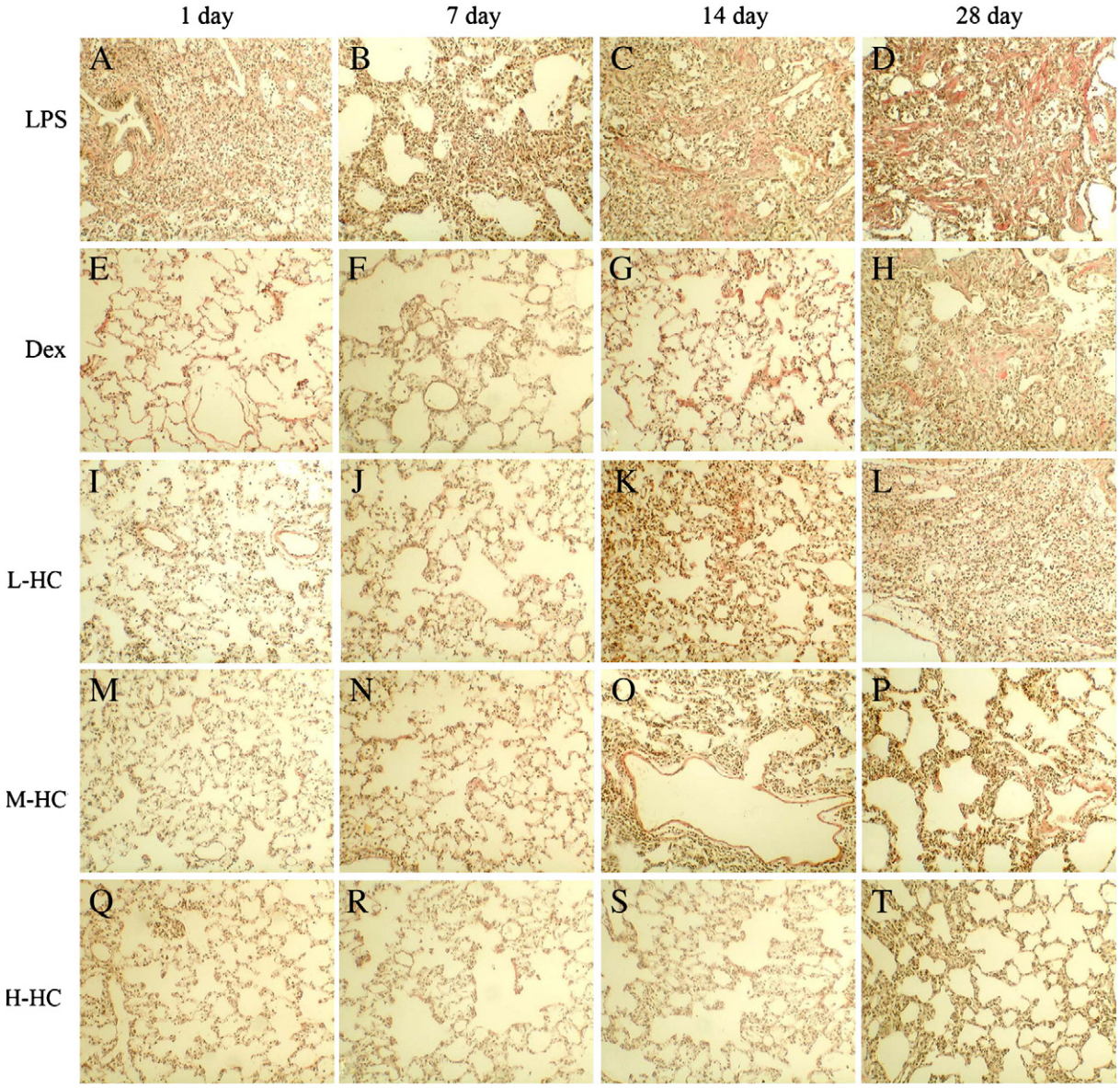

Fig. 2. Collagen fibers with van Gieson staining. The collagen fibers are red, and the cells are brownish-black. LPS group on day 1 (A, ×100): the number of inflammatory cells in the alveolar spaces increased, the pulmonary interstitium was destroyed, and collagen fibers ruptured, indicating pulmonary exudative inflammation. LPS on day 7 (B, ×200): the pulmonary interstitium broadened significantly, the number of collagen fibers increased, and the pulmonary interstitium was restructured. LPS on days 14–28 (C, D, ×100): the red collagen fibers thickened dramatically and formed bunches or sheets indicative of pulmonary fibrosis. Dex inhibited inflammation exudation dramatically. On day 1 (E, ×100), the collagen fibers in the alveolar spaces were normal, the alveoli were intact, and there were fewer inflammatory cells in the interstitial space and alveolar spaces. Dex on days 7 and 14 (F, G, ×100): the pulmonary interstitium thickened, the inflammatory exudation in alveolar spaces increased, and the interstitial collagen fibers thickened. Dex on day 28 (H, ×100): the interstitial space thickened and consolidated significantly, and the alveolar spaces narrowed. HC groups on day 1 (I, M, Q, × 100): the interstitial space was normal. HC on days 7 to 28 (N, ×100): the pulmonary interstitial collagen fibers proliferated persistently, and the interstitial space thickened. L-HC group on day 28 (L, ×100): the number of interstitial cells increased, and the alveoli narrowed. M-HC and H-HC groups (P, T, ×100): the interstitial space thickened, and the number of collagen fibers increased significantly, but the alveoli were normal.

to the first RPF stage. Therefore, the down-regulation of Smad4 expression on days 1–7 in the HC groups might be an important molecular mechanism through which the HC vapor extract inhibits RPF.

Smad7 is the antagonistic Smad of Smad2/3 signaling. The western blotting (Fig. 4) and immunohistochemical (Supplement Fig. 3) results showed that Smad7 expression was higher on day 7 than on day 1 in all groups and was weak in the LPS and Dex groups on day 28; however, the expression remained high in the HC groups in a dose-dependent manner. This suggests that the HC vapor extract up-regulates Smad7.

3.5 . The active ingredients of the HC vapor extract include 4-terpineol, α-terpineol, L-bornyl acetate and methyl-n-nonyl ketone

We tested three groups of HC vapor extract using GC–MS (Fig. 5) and found that the active ingredients of HC vapor extract were composed of 4-terpineol (42.77 ± 5.61%), α-terpineol (16.55 ± 3.44%), L-bornyl acetate (2.60 ± 0.21%) and methyl-n-nonyl ketone (38.08 ± 2.00%). The HC content of these four components was stable across groups, accounting for 80.61–91.68% of the total amount, with an average content of 86.99%. In contrast, other components were

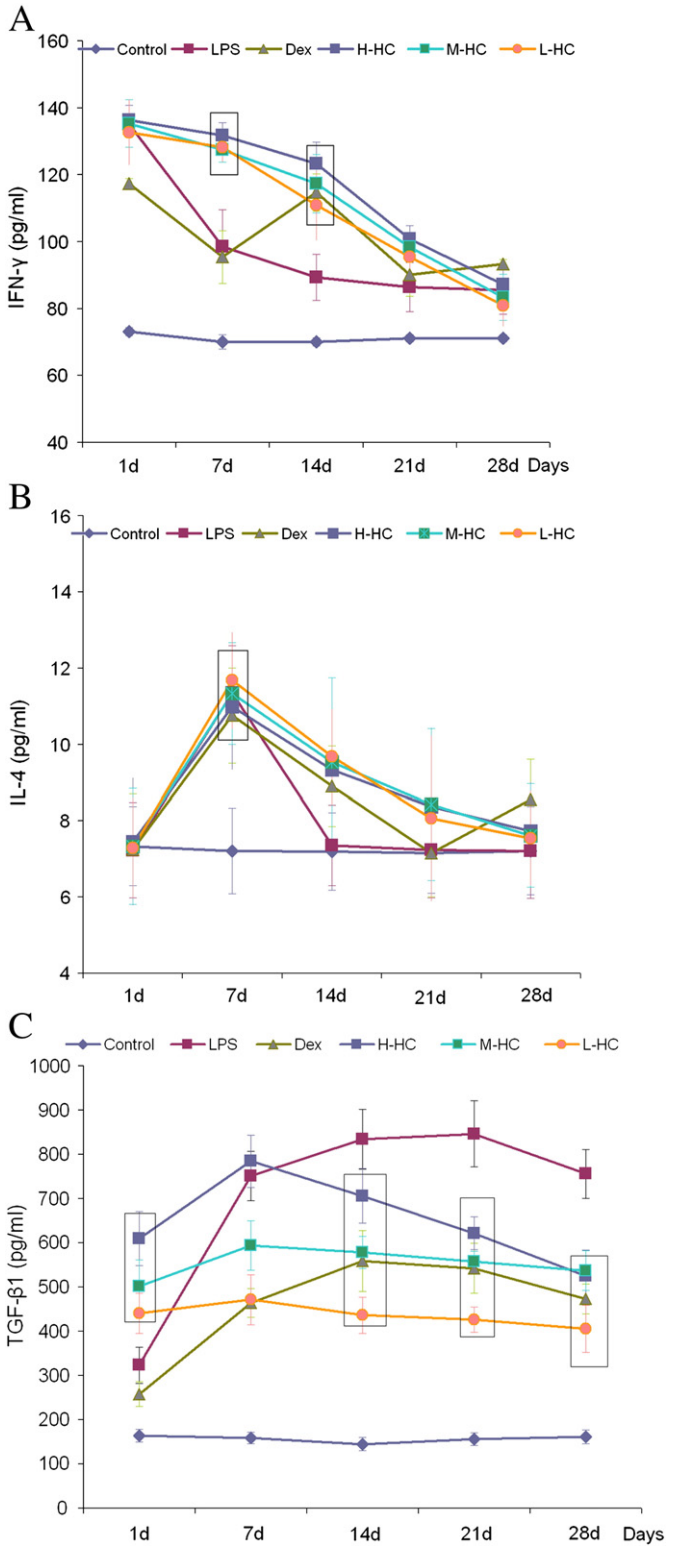

Fig. 3. ELISA assay of Th1/Th2 serum cytokines (IFN-γ, IL-4 and TGF-β1): the statistical analysis is shown in Supplemental Tables 7–9. The boxes in Fig. 4 highlight the dose-dependent effects of HC. There is a significant difference between the HC groups. (A) Concentration of IFN-γ (pg/ml); (B) concentration of IL-4 (pg/ml); (C) concentration of TGF-β1 (pg/ml).

present in smaller quantities (13.02 ± 5.72%) and were not as stable across the groups, suggesting that they are not responsible for the main pharmacological effect. Therefore, we choose α-terpineol, L-bornyl acetate and methyl-n-nonyl ketone to study the potential pharmacological mechanism of the four components. Some reports [17] have proposed that sodium houttuyfonate (SH) was the effective component of HC. Thus, we used HC as the positive control. RAW264.7 and NIH/3T3 cells are typical immune and fibroblast cells, respectively. These are two important cell types involved in damage and repair. We observed the viability of RAW264.7 and NIH/3T3 cells after 24 h, 48 h, and 72 h of treatment with the HC vapor extract (10%, 30%, 50%; HC), α-terpineol (0.1 mg/ml, 0.5 mg/ml, 1 mg/ml), L-bornyl acetate (2.5 μl/ml, 5 μl/ml, 10 μl/ml), methyl-n-nonyl ketone (1 μl/ml, 2 μl/ml, 4 μl/ml) and SH (32 μg/ml, 64 μg/ml, 128 μg/ml). After 48 h, LPS (100 ng/ml), HC vapor extract, SH and α-terpineol inhibited the viability of RAW264.7 cells, but L-bornyl acetate enhanced viability significantly and dose-dependently (Fig. 6A). In addition, HC vapor extract, α-terpineol and L-bornyl acetate inhibited the viability of NIH/3T3 cells significantly and dose-dependently (Fig. 6B). We also observed the viability of cells 24 h and 72 h after being treated with LPS or without treatment with LPS. The results show that the HC vapor extract can inhibit the viability of RAW264.7 and NIH/3T3 cells.

3.6 . HC dose-dependently inhibited the expression of TGF-β1 and enhanced IFN-γ in NIH/3T3

We used ELISA to analyze the concentrations of TGF-β1 and IFN-γ in the NIH/3T3 supernatant after 48 h of treatment with LPS (Fig. 7A and B). HC and α-terpineol up-regulated IFN-γ expression, but L-bornyl acetate inhibited it significantly and dose-dependently. HC inhibited TGF-β1 expression, but SH up-regulated it significantly and dose-dependently. The results suggest that the HC vapor extract inhibits TGF-β1 and enhances IFN-γ secretion from NIH/3T3 cells in a dose-dependent manner.

4 . Discussion

In this investigation, we applied the volatile extract of HC to the RPF rat model and found that HC could repair RPF through up-regulating IFN-γ and inhibiting the TGF-β1/Smad pathway. Moreover, we found that the volatile components of the HC vapor extract were mainly composed of 4-terpineol, α-terpineol, L-bornyl acetate and methyl-n-nonyl ketone. HC inhibited the viability of NIH/3T3 and RAW264.7 cells. HC inhibited TGF-β1 secretion and enhanced IFN-γ secretion from NIH/3T3 cells, suggesting that these effects might contribute to the results observed *in vivo*. Interestingly, α-terpineol, L-bornyl acetate and SH had diverse effects on NIH/3T3 and RAW264.7 cells, suggesting that the volatile extract of HC has complicated mechanisms of action through which it affects ALI and RPF.

Recent studies have found that the active ingredients of the HC water extract, such as α-terpineol and L-bornyl acetate, had strong anti-tumor, anti-virus, anti-pneumonia and anti-pulmonary fibrosis effects [10,18]. α-Terpineol has been suggested as a potential anticancer agent that suppresses NF-κB signaling [19], and L-bornyl acetate has been shown to inhibit nitric oxide (NO) and prostaglandin E2 (PGE2) production in lipopolysaccharide (LPS)-activated RAW264.7 macrophages [20]. An HC water extract remarkably improved the morphological appearance of the lung in bleomycin-treated rats and exhibited a protective effect against bleomycin-induced pulmonary fibrosis [21]. Our investigation found that α-terpineol dose-dependently enhanced IFN-γ, but L-bornyl acetate had the opposite effect (Fig. 7A). The HC vapor extract inhibited TGF-β1, while SH did not (Fig. 7B), suggesting that α-terpineol, L-bornyl acetate and SH might have different pharmacological actions on ALI and AFP.

It has been suggested that Th2 polarization might be a necessary condition of ALI-induced fibrosis [16,22]. In the LPS group, we observed Th2 polarizations. IFN-γ expression decreased consistently, and IL-4 and TGF-β1 expression increased consistently, which further induced RPF. The period from days 3 to 7 constituted the first stage of RPF, and the second stage of RPF was from days 14 to 21. HC and Dex

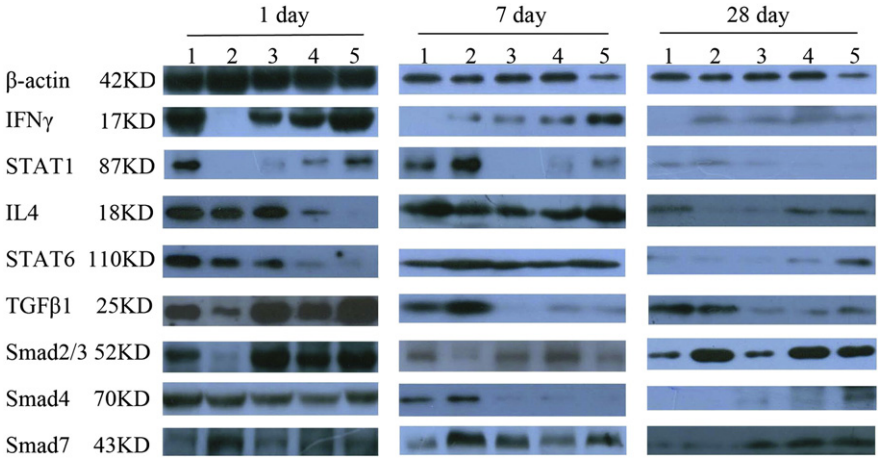

Fig. 4. Western blotting results for β-actin, IFN-γ, STAT-1, IL-4, STAT6, TGF-β1, Smad2/3, Smad4 and Smad7. Lane 1: LPS group; lane 2: Dex group; lane 3: L-HC group; lane 4: M-HC group; lane 5: H-HC group.

did not show obvious differences in anti-inflammatory and anti-fibrosis effects on days 3–7, and HC showed better anti-inflammatory and anti-fibrosis effects than Dex on days 14–21. Compared with Dex, HC appropriately improved immune stress status by up-regulating the lympocytes/mononuclear phagocytes ratio on day 7, which might be more advantageous (Fig. 1A and B).

A

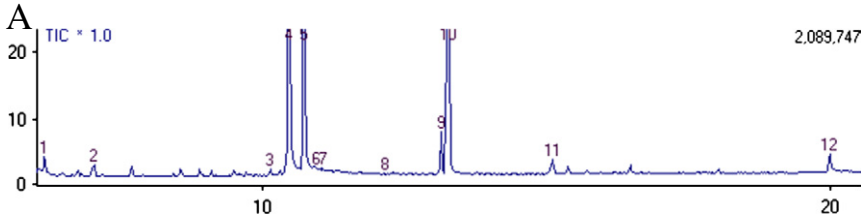

4. 4-terpineol; 5.α-terpineol; 9. L-bornyl acetate; 10. methyl-n-nonyl ketone.

B

PKNO	R.TIME	I.TIME	F.TIME	A/H(sec)	AREA	HEIGHT	MARK	%Total	NAME
1	6.177	6.125	6.333	2.772	626563	226058	V	1.23	
2	7.052	6.992	7.408	4.084	589687	144389	S	1.15	
3	10.15	10.067	10.367	7.028	679294	96655	V	1.33	
4	10.481	10.4	10.65	2.271	18735169	8250328	V	36.64	4-terpineol
5	10.742	10.65	10.908	2.72	9284644	3413358	V	18.16	α-terpineol
6	10.974	10.908	11.033	7.212	780826	108260	V	1.53	
7	11.077	11.033	11.167	6.558	664695	101359	V	1.3	
8	12.164	11.842	12.192	19.107	603185	31569	V	1.18	
9	13.156	13.008	13.233	2.507	1455037	580361	V	2.85	L-bornyl acetate
10	13.279	13.233	30.55	1.937	15870746	8194021	VS	31.04	methyl-n-nonyl ketone
11	15.113	15.025	15.15	3.377	729418	215967	VT	1.43	
12	19.993	19.867	20.067	4.077	1113569	273134	VT	2.18	

C

NAME	%Total (Mean)	SD
4-terpineol	29.62	6.16
α-terpineol	22.26	5.19
L-bornyl acetate	2.35	0.51
methyl-n-nonyl ketone	32.76	8.73
others	13.02	5.72
%Total	100.01	

Fig. 5. Active ingredients of the HC vapor extract analyzed by GC–MS. Three groups of HC vapor extracts were collected though distillation and redistillation and were analyzed by an Agilent 6890 N + 5973 N GC–MS (USA) with a 30 m × 0.25 mm × 0.25 μm DB-1MS quartz micro capillary chromatographic column (Agilent J&W Scientific). The diluted samples (1.0 μl, 1/100 v/v in ethyl acetate) were injected manually in the split mode. The major components of the HC vapor extract were identified by co-injection with standards and confirmed with Kovats indices using the Wiley (V. 7.0) and National Institute of Standards and Technology (NIST) V2.0 GC–MS library. The relative concentration of each compound in essential oil was quantified based on the peak area integrated by the analysis program. A: the raw GC–MS figure for one group; B: the raw data (based on A) from GC–MS for one group; C: the statistical data for one group.

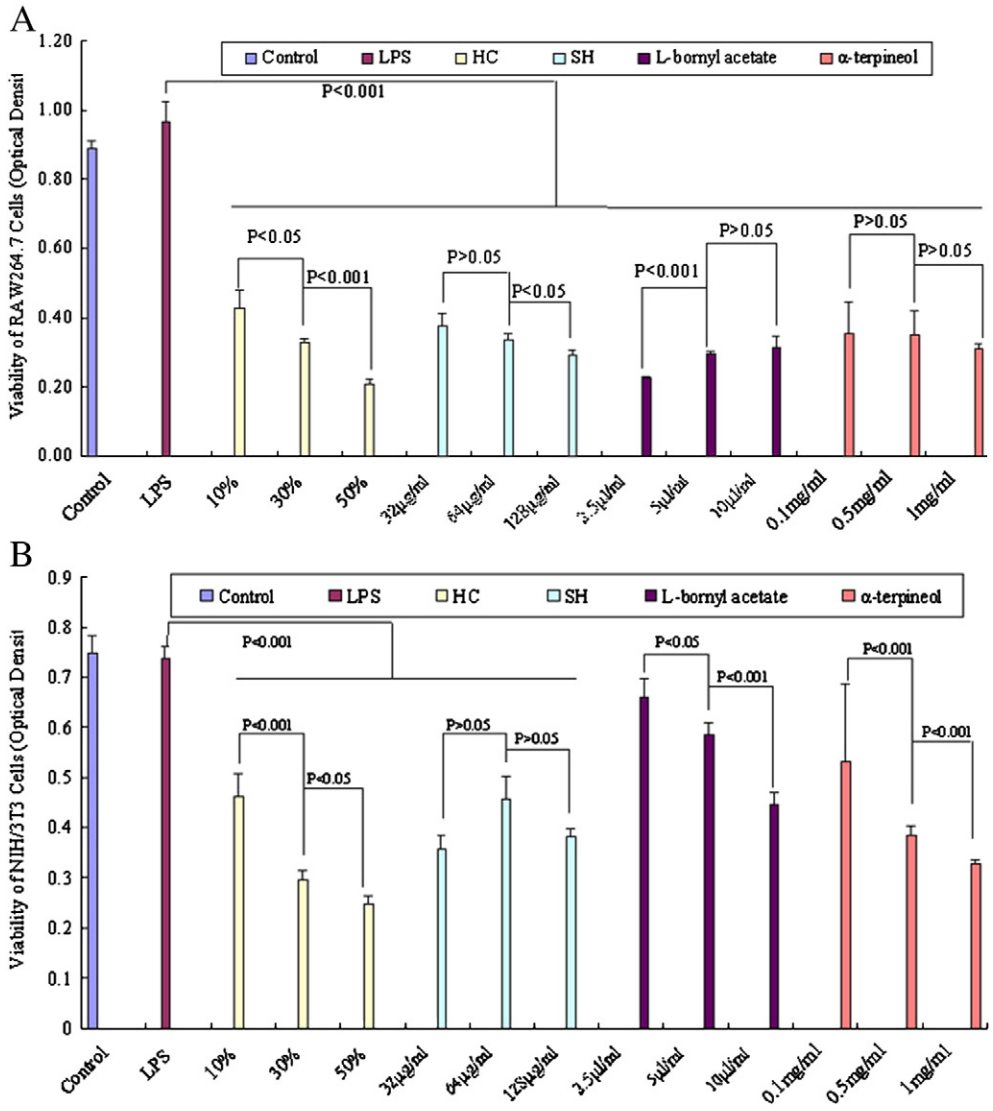

Fig. 6. HC and its active ingredients affected the viabilities of RAW264.7 and NIH/3T3 cells after a 48 h treatment with LPS (100 ng/ml). MTT was used to assess cell viability A: viability of RAW264.7 cells; B: viability of NIH/3T3 cells.

IFN-γ, as a Th1 cytokine with multiple functions, has pro-inflammatory, anti-viral and anti-fibrosis effects [23,24]. IFN-γ inhibited influenza virus type A [25] and SARS-CoV replication [24] *in vitro*, suggesting that up-regulating IFN-γ may increase the survival of SARS patients. IFN-γ expression declined in the LPS group, suggesting that the immune system was suppressed to induce RPF. The HC vapor extract increased IFN-γ expression on days 7–21, and the results from the NIH/3T3 cells showed that α-terpineol might be the active ingredient of the HC vapor extract that up-regulates IFN-γ expression. The HC-induced up-regulation of IFN-γ expression was not accompanied by an up-regulation in STAT1 expression, suggesting that the HC vapor extract might inhibit the pro-inflammatory STAT1 pathway. Thus, the up-regulation of IFN-γ might be an important mechanism through which HC reduces RPF.

TGF-β1, as a Th2 cytokine with multiple functions, plays an important role in pulmonary fibrosis [26–28]. In ALI, TGF-β1 inhibited inflammation and improved repair. In RPF, TGF-β1 was up-regulated further to prompt fibrosis, and Smad4 and Smad7 were suggested to be involved in crucial molecular mechanisms of RPF [16]. In our investigation, the HC vapor extract inhibited the TGF-β1 signal *via* the Smad2/3 pathway. At the same time, Smad4 was expressed weakly and Smad7 expression increased. Our results suggest that the HC vapor extract repaired RPF through inhibiting the TGF-β1/Smad pathway.

Additionally, some researchers have stated that the over-expression of Smad7 antagonizes TGF-β1 signaling [29]. Smad7 reduces the expression of TGF-β1-induced CTGF, which has a positive correlation with fibrosis [30]. IFN-γ promotes the activation of the JAK1/STAT1 pathway, which inhibits TGF-β1 signaling and subsequent collagen production through a Smad7-dependent pathway [31].

In summary, our investigation shows that the pharmacologically active ingredients of HC vapor extract might be α-terpineol and L-bornyl acetate, which reduced ALI and RPF, and that IFN-γ and the TGF-β1/Smad pathway might be the pharmacological targets of HC.

Supplementary data related to this article can be found online at http://dx.doi.org/10.1016/j.intimp.2012.03.011.

Competing interests

The authors declare that they have no competing interests.

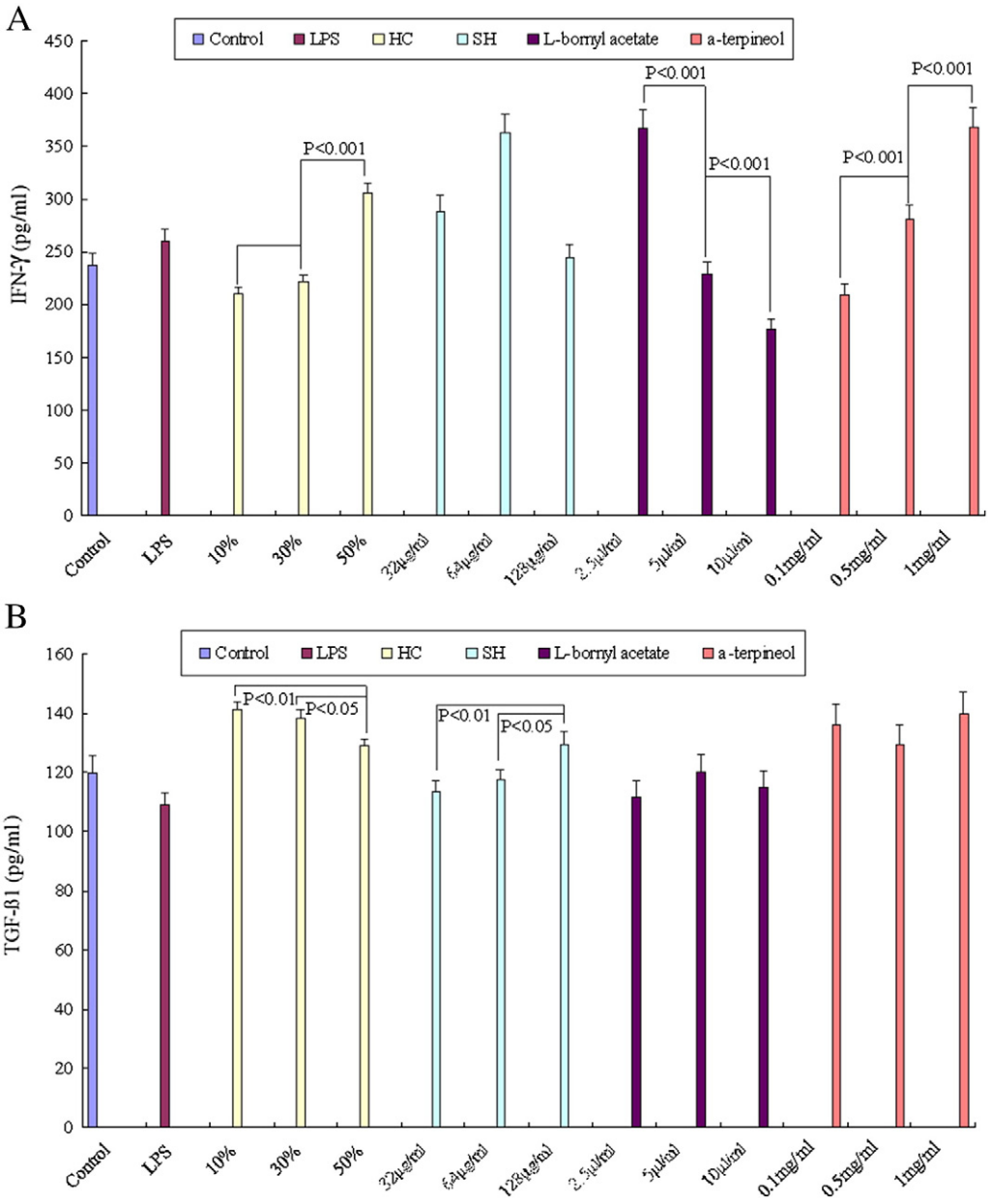

Fig. 7. HC and its active ingredients affected the expression of IFN-γ and TGF-β1 in NIH/3T3 cells after 48 h of treatment with LPS (100 ng/ml). Expression was measured using an ELISA assay. A: concentration of IFN-γ (pg/ml); B: concentration of TGF-β1 (pg/ml).

Acknowledgments

This work was supported by the National Natural Science Foundation of China (grant no. 30572454, no. 81072908 and no. 81173377) and the Guangdong Provincial Science & Technology Project (no. 2009B030801283). We thank Dr. Qiduan Wu and Yongqi Fang from the First Affiliated Hospital to Guangzhou University of Chinese Medicine for their helpful assistance with GC–MC.

References

[1] Kolb MR, Richeldi L. Viruses and acute exacerbations of idiopathic pulmonary fibrosis: rest in peace? Am J Respir Crit Care Med 2011;183:1583–4.
[2] de Boer K, Vandemheen KL, Tullis E, et al. Exacerbation frequency and clinical outcomes in adult patients with cystic fibrosis. Thorax 2011;66:680–5.
[3] World Health Organization. The World Health Report 2007—A safer future: global public health security in the 21st century vi.
[4] Dos Santos CC. Advances in mechanisms of repair and remodelling in acute lung injury. Intensive Care Med 2008;34:619–30.
[5] Chambers RC. Procoagulant signalling mechanisms in lung inflammation and fibrosis: novel opportunities for pharmacological intervention? Br J Pharmacol 2008;153:s367–78.
[6] Budinger GR, Chandel NS, Donnelly HK, et al. Active transforming growth factor-beta1 activates the procollagen I promoter in patients with acute lung injury. Intensive Care Med 2005;31:121–8.
[7] Hayashi K, Kamiya M, Hayashi T. Virucidal effects of the steam distillate from *Houttuynia cordata* and its components on HSV-1, influenza virus, and HIV. Planta Med 1995;61(3):237–41.
[8] Chinese Thoracic Society, CMA. Consensus of the clinical management of severe acute repiratory syndrome. Chin J Tuberc Respir Dis 2003;26:323–4.
[9] Lau KM, Lee KM, Koon CM, Cheung CS, Lau CP, Ho HM, et al. Immunomodulatory and anti-SARS activities of *Houttuynia cordata*. J Ethnopharmacol 2008;118(1):79–85.
[10] Lee JS, Kim IS, Kim JH, Kim JS, Kim DH, Yun CY. Suppressive effects of *Houttuynia cordata* Thunb (Saururaceae) extract on Th2 immune response. J Ethnopharmacol 2008;117(1):34–40.
[11] Ren X, Sui X, Yin J. The effect of *Houttuynia cordata* injection on pseudorabies herpesvirus (PrV) infection *in vitro*. Pharm Biol 2011 Feb;49(2):161–6.
[12] Li W, Zhou P, Zhang Y, He L. *Houttuynia cordata*, a novel and selective COX-2 inhibitor with anti-inflammatory activity. J Ethnopharmacol 2011 Jan 27;133(2):922–7.
[13] Zeng Zhong-Da, Liang Yi-Zeng, Zhang Ting, Chau Foo-Tim, Wang Ya-Li. Orthogonal projection (OP) technique applied to pattern recognition of fingerprints of

the herbal medicine *Houttuynia cordata* Thunb. and its final injection products. Anal Bioanal Chem 2006;385:392–400.
[14] Shin S, Joo SS, Jeon JH, Park D, Jang MJ, Kim TO, et al. Anti-inflammatory effects of a *Houttuynia cordata* supercritical extract. J Vet Sci Sep. 2010;11(3):273–5.
[15] Tan Z, Chao Z, Sui Y, Liu H, Wu X, Sun J, et al. Effect of Tween 80 on yuxingcao injection and volatile oils from *Houttuynia cordata*. Zhongguo Zhong Yao Za Zhi Jan. 2011;36(2):175–9 [Article in Chinese].
[16] Li H, Du S, Yang L, Chen Y, Huang W, Zhang R, et al. Rapid pulmonary fibrosis induced by acute lung injury *via* a lipopolysaccharide three-hit regimen. Innate Immun 2009;15:143–54.
[17] Liu G, Xiang H, Tang X, Zhang K, Wu X, Wang X, et al. Transcriptional and functional analysis shows sodium houttuyfonate-mediated inhibition of autolysis in *Staphylococcus aureus*. Molecules 2011 Oct 21;16(10):8848–65.
[18] Gertsch J. How scientific is the science in ethnopharmacology? Historical perspectives and epistemological problems. J Ethnopharmacol 2009;122(2):177–83.
[19] Hassan SB, Gali-Muhtasib H, Göransson H, Larsson R. Alpha terpineol: a potential anticancer agent which acts through suppressing NF-kappaB signalling. Anticancer Res 2010;30(6):1911–9.
[20] Tung Yu-Tang, Chua Meng-Thong, Wang Sheng-Yang, Chang Shang-Tzen. Anti-inflammation activities of essential oil and its constituents from indigenous cinnamon (*Cinnamomum osmophloeum*) twigs. Bioresour Technol 2008;99:3908–13.
[21] Ng LT, Yen FL, Liao CW, Lin CC. Protective effect of *Houttuynia cordata* extract on bleomycin-induced pulmonary fibrosis in rats. Am J Chin Med 2007;35(3): 465–75.
[22] Ministry of Health of the People's Republic of China. Discharge guideline for patients diagnosed as severe acute respiratory syndrome; 2003.
[23] Shea LM, Beehler C, Schwartz M, Shenkar R, Tuder R, Abraham E. Hyperoxia activates NF-kappaB and increases TNF-alpha and IFN-gamma gene expression in mouse pulmonary lymphocytes. J Immunol 1996;157:3902–8.
[24] Sainz Jr B, Mossel EC, Peters CJ, Garry RF. Interferon-beta and interferon-gamma synergistically inhibit the replication of severe acute respiratory syndrome-associated coronavirus (SARS-CoV). Virology 2004;329:11–7.
[25] Khoufache K, LeBouder F, Morello E, Laurent F, Riffault S, Andrade-Gordon P, et al. Protective role for protease-activated receptor-2 against influenza virus pathogenesis *via* an IFN-gamma-dependent pathway. J Immunol 2009;182:7795–802.
[26] Attisano L, Wrana JL. Signal transduction by the TGF-beta superfamily. Science 2002;296:1646–7.
[27] Frank S, Madlener M, Werner S. Transforming growth factors beta1, beta2, and beta3 and their receptors are differentially regulated during normal and impaired wound healing. J Biol Chem 1996;271:10188–93.
[28] Grande JP. Role of transforming growth factor-beta in tissue injury and repair. Proc Soc Exp Biol Med 1997;214:27–40.
[29] Nakao A, Fujii M, Matsumura R, Kumano K, Saito Y, Miyazono K, et al. Transient gene transfer and expression of Smad7 prevents bleomycin-induced lung fibrosis in mice. J Clin Invest 1999;104:5–11.
[30] Xie S, Sukkar MB, Issa R, Khorasani NM, Chung KF. Mechanisms of induction of airway smooth muscle hyperplasia by transforming growth factor-beta. Am J Physiol Lung Cell Mol Physiol 2007;293:L245–53.
[31] Ulloa L, Doody J, Massague J. Inhibition of transforming growth factor-beta/Smad signalling by the interferon-gamma/STAT pathway. Nature 1999;397:710–3.